



Integration of geochronological, lithofacial and paleontological data to refine the context of the Marifil Complex (Jurassic), Río Negro, Argentina

Cecilia PAVÓN PIVETTA^{1,2}, Juan E. DI NARDO^{1,3}, Leonardo BENEDINI^{1,2}, Daniel GREGORI^{1,2}, Josefina BODNAR^{4,5}, Mercedes V. BARROS^{1,2}, Leonardo STRAZZERE^{1,2}, Paulo MARCOS⁶, Anderson COSTA DOS SANTOS^{7,8}, Mauro C. GERALDES⁷

¹Departamento de Geología, Universidad Nacional del Sur (UNS), Bahía Blanca, Argentina.

²Instituto Geológico del Sur (INGEOSUR), Universidad Nacional del Sur (UNS)-CONICET, Bahía Blanca, Argentina.

³Comisión de Investigaciones Científicas (CIC) de la provincia de Buenos Aires.

⁴Consejo Nacional de Investigaciones Científicas y Técnicas (CONICET), Argentina.

⁵División Paleobotánica, Facultad de Ciencias Naturales y Museo, Universidad Nacional de La Plata, Paseo del Bosque s/n, B1900FWA La Plata, Argentina.

⁶Instituto de Investigación en Paleobiología y Geología (IIPG), UNRN-CONICET, Av. Julio A. Roca 1242, R 8332 EXZ General Roca, Río Negro, Argentina

⁷Departamento de Geologia Regional, Faculdade de Geologia, Universidade do Estado do Rio de Janeiro, Rua São Francisco Xavier 534, Sala 3107F Maracanã, Brazil

⁸Geobiotec, Departamento de Geociências, Universidade de Aveiro, Aveiro, Portugal.

Autor correspondiente: cpavonpivetta@gmail.com

Editor: Susana E. Damborenea

Recibido: 15 de octubre de 2024

Acceptado: 8 de diciembre de 2024

ABSTRACT

In northeastern Patagonia, outcrops of the Marifil Complex located 3 km north of Mina Delta XXI expose a succession of volcanoclastic and sedimentary rocks 160 m thick. This succession, along with other correlatable deposits, was previously mapped as undifferentiated ignimbrites, tuffs, and sandstones in recent regional geological surveys. The Marifil Complex in the study area comprises ten distinct lithofacies, including paraconglomerates forming the basal layer of the volcano-sedimentary succession; coarse-grained arkosic sandstones; volcanic sandstones and siltstones containing fossil flora; mixed volcanic-clastic rocks; massive brecciated and bituminous limestones; massive lapilli-rich and crystal-rich eutaxitic tuffs; and porphyritic rhyolites that intrude the other facies. The volcano-sedimentary succession studied is interpreted as having been deposited in a small lacustrine basin adjacent to an explosive volcanic center. The macrofloral assemblage includes equisetalean stems assigned to *Equisetites* sp., conifer vegetative and reproductive structures (*Pagiophyllum* spp., a probable bract/seed-scale complex and a probable pollen cone), and an incomplete leaf fragment with reticulate venation of uncertain affinities. Additionally, a gymnosperm pollen grain assigned to *Inaperturopollenites indicus* Srivastava was identified from the same levels. The age of this geological unit, determined by U-Pb zircon geochronology, is 189.5 ± 2.2 Ma, constraining the deposition and associated paleoflora to the Sinemurian-Pliensbachian boundary. These volcanic and volcano-sedimentary deposits are associated with the development of an extensional basin, possibly linked to the breakup of Gondwana.

Keywords: *Mina Delta XXI, volcano-sedimentary lithofacies, lacustrine basin, paleoflora, U-Pb zircon geochronology, Sinemurian-Pliensbachian boundary.*

RESUMEN

Integración de datos geocronológicos, litofaciales y paleontológicos para precisar el contexto del Complejo Marifil (Jurásico), Río Negro, Argentina. (Jurásico Medio).

En el noreste de la Patagonia, los afloramientos del Complejo Marifil, ubicados a tres kilómetros al norte de Mina Delta XXI exponen una sucesión de rocas volcanoclásticas y sedimentarias con un espesor de 160 m. Esta sucesión, junto con otros depósitos correlacionables, fue previamente caracterizada como ignimbritas, tobas y areniscas no diferenciadas en relevamientos geológicos regionales recientes. En el área de estudio, el Complejo Marifil comprende diez litofacies distintas: paraconglomerados; areniscas arcóscicas masivas de grano grueso; areniscas y pelitas volcánicas con flora fósil, rocas volcanoclásticas de mezcla que incluyen componentes terrígenos de tamaño limo y arena, componentes calcáreos y volcánicos; calizas masivas brechadas y bituminosas, tobas masivas eutaxíticas ricas en lapilli y cristales; y riolitas porfíricas que intruyen toda la sucesión. La asociación macroflorística incluye tallos de equisetales asignados a *Equisetites* sp., estructuras vegetativas y reproductivas de coníferas (*Pagiophyllum* spp., un probable complejo bráctea-escama-óvulo y un probable cono polínico), y un fragmento incompleto de hoja con venación reticulada de afinidad incierta. Además, se identificó un grano de polen de gimnosperma asignado a *Inaperturopollenites indicus* Srivastava en los mismos niveles. Se interpreta que esta sucesión volcano-sedimentaria se depositó en una pequeña cuenca lacustre adyacente a un centro volcánico explosivo. La edad de esta secuencia, determinada mediante geocronología U-Pb en circones, es de $189,5 \pm 2,2$ Ma, lo que sitúa su depósito y paleoflora asociada en el límite Sinemuriano-Pliensbachiano. Estos depósitos volcánicos y volcano-sedimentarios están vinculados al desarrollo de una cuenca extensional, posiblemente relacionada a la fragmentación de Gondwana.

Palabras clave: Mina Delta XXI, Litofacies volcano-sedimentarias, cuenca lacustre, paleoflora, geocronología U-Pb en circones, límite Sinemuriano-Pliensbachiano.

INTRODUCTION

In recent years, numerous studies in northern Patagonia have documented the presence of fossil flora in spatially confined volcano-sedimentary successions linked to Early Jurassic volcanism (Ferello, 1947; Herbst, 1966; Escapa et al. 2008; Morel et al. 2013; Strazzere et al. 2019; Sagasti et al. 2019; Falco et al. 2021). The epiclastic and pyroclastic deposits, interbedded with volcanic rocks, provide evidence of the significant development of confined continental basins associated with intense volcanic activity.

The geological configuration of Gondwana during the Early Jurassic includes ample evidence of the magmatism developed in South Africa, Antarctica, Australia-New Zealand, and South America (Cox, 1992; Encarnación et al. 1996; Riley and Knight, 2001; Storey et al. 2001). The origin of magmatism is widely controversial. The earliest data related to the presence of mantle plumes were located beneath South Africa and Antarctica at c. 182 Ma (Riley and Knight, 2001). Jurassic igneous rocks of the Marifil Complex in the Chon Aike magmatic province include volcanic events V1, V2 and V3 (Pankhurst et al. 2000). Current proposals (Pavón Pivetta et al. 2020) indicate the presence of a V0 volcanic event with radiometric ages of 190 ± 2 Ma and geochemically related to the possible presence of a flat slab break-off produced at the same time (Gianni et al. 2018, 2019 and 2023; Navarrete et al. 2019 a and b). In relation to these differences in the plate subduction angle and presence of epithermal veins, several authors (Pavón Pivetta et al. 2020 and 2024; Pugliese et al. 2021) proposed the relationship of low sulfidation epithermal deposits with the V0 volcanic event. Other authors indicated that in the

NW of northern Patagonia, the first volcanic event is from the late Sinemurian, which developed maar-diatremes, dike intrusions, and related continental sedimentation in a pull-apart basin (Benedini et al. 2022).

In northeastern Patagonia (Fig.1), the Early Jurassic volcanic and subvolcanic igneous rocks with extensive areal distribution were named the Marifil Formation (Malvicini and Llambías 1974). Subordinate sedimentary and volcanoclastic rocks were described and incorporated to define the Marifil Complex (Cortés, 1981; Busteros et al. 1998). Within this lithostratigraphic unit, sedimentary and volcano-sedimentary facies were grouped under the name Puesto Piris Formation (Nuñez et al. 1975; Cortés 1981; González et al. 2017a; Strazzere et al. 2019).

Nuñez et al. (1975) mentioned the presence of leaf remains belonging to the genera *Otozamites*, *Dictyozamites*, and *Ptilophyllum* in the Marifil Complex, which, in association with freshwater crustaceans (*Estheria*), were assigned to the Early to Middle Jurassic. Subsequent isotopic dating performed on tuffs and volcanic rocks has made it possible to refine its age to the Early Jurassic (Cortés 1981; Chernicoff et al. 2017; Strazzere et al. 2019; Pugliese et al. 2021; González et al. 2022 and references therein).

The volcano-sedimentary succession in the study area crops out 20 km south of the Sierra Grande locality and covers an area of approximately 12 km². The most recent regional maps indicate the presence of undifferentiated outcrops of ignimbrites, tuffs, and sandstones attributed to the Marifil Complex (Busteros et al. 1998). The sedimentary and volcano-sedimentary facies were briefly described as thin levels of locally important clastic and chemical sedimentary rocks,

interbedded with pyroclastic horizons. Despite their limited thickness and areal extent, these rocks are powerful correlation elements, and their fossil content is of great importance both for determining the age of the units and for correlations at local and global scales (González et al. 2017b).

Recent explorations have allowed detailed mapping and precise characterization of the volcanic-sedimentary lithofacies, which were previously indistinguishable in regional geological surveys. A fossil plant assemblage was recovered from one of the mapped levels and these strata are referred to here as the Puesto Piris Formation.

This study aims to carry out a stratigraphic and paleontological analysis of the volcano-sedimentary lithofacies in order to reconstruct the sedimentary environments associated with Jurassic volcanism. It presents a new U-Pb isotopic age from magmatic zircon grains that emphasizes the importance of the Puesto Piris Formation for understanding the sedimentary evolution of northern Patagonia during the Early Jurassic. The Mina Delta XXI area has significant potential for the discovery of new floristic assemblages, offering valuable insights into the ecosystems and biodiversity of northern Patagonia during the Early Jurassic. Although this study provides a preliminary overview, future research will address a more detailed analysis of the paleobotanical content.

GEOLOGICAL SETTING

The study area is located north of the Mina Delta XXI area, Río Negro Province, in the Northeastern Patagonian Region (Fig. 1). The basement rocks of the volcano-sedimentary sequence under study comprise the El Jagüelito Formation, Sierra Grande Formation, and Permian granites. The Cambrian El Jagüelito Formation (Ramos 1975; Giacosa 1987) crops out five km to the northwest, outside the study area, and includes schist, orthogneiss and paragneiss, amphibolite, para-amphibolite, marbles and granitoids. The Ordovician to Devonian Sierra Grande Formation (Valvano 1954; Cortés 1979) is an iron-bearing unit that includes the MCC Minera Sierra Grande iron mine and is exposed in the northern sector of the study area. In the vicinity of the iron mine, the Permian granites are mapped as the Laguna Medina Pluton and are part of the Permian-Triassic Pailemán Plutonic Complex (Busteros et al. 1998). We assume that the granite in Mina Delta XXI is part of the Laguna Medina Pluton.

The Jurassic rocks were originally defined as the Marifil Formation, including only the volcanic rocks (Malvicini and Llambías 1974), and later redefined as the Marifil Complex (Cortés 1981) to include three units separated by unconform-

ities: Puesto Piris, Aguada de Bagual, and La Porfía formations. The basal section of Marifil Complex consists of sedimentary rocks called the Puesto Piris Formation (Nuñez et al. 1975 and Cortés 1981). These authors described a succession of alternating grey and red conglomerate beds covered by thick pyroclastic-flow deposits in the upper part of the unit.

Nuñez et al. (1975) proposed a Triassic age for the Puesto Piris Formation, distinguishing its lithologies from those of the overlying, unconformable volcanic, sedimentary, and volcano-sedimentary deposits, assigned at that time to the Marifil Formation. Nuñez et al. (1975) identified at least four fossiliferous levels in the outcrops of the Marifil Complex sequence, located about two km from the railway between Viedma and Bariloche (km 275). They reported the presence of leaves attributed to the genera *Otozamites*, *Dictyozamites*, and *Ptilophyllum*, suggesting an Early to Middle Jurassic age. Freshwater crustaceans belonging to the genus *Estheria* were also reported.

In the Puesto Piris area, 100 km north-northwest of the study area, Strazzere et al. (2019) performed a facies analysis of the Puesto Piris Formation. Active volcanism coeval with sedimentation was inferred from reworked massive tuffs and volcanic-rich deposits (juvenile components) interbedded with the sedimentary facies. Fossil plant remains belonging to equisetaleans, conifers and tree ferns, as well as the green algae *Botryococcus*, have been found in some of the strata. Isotopic dating indicates a Sinemurian age for the sedimentation, fossil plant assemblage and volcanism (Strazzere et al. 2019).

In the Puesto Perdomo area, 50 km west of the study area, Díaz-Martínez et al. (2017) reported the discovery of dinosaur footprints in sedimentary rocks of Early Jurassic age associated with the Marifil Complex. They also mentioned the presence of plant remains, attributed to equisetals, a few meters above the horizons in which the footprints were found.

In the case of the Mina Delta XXI, Zanettini (1981) indicated high-energy continental deposits and attributed them to a post-orogenic environment with tectonic instability, dominated by scarce transport of basal lithofacies.

MATERIALS AND METHODS

Lithofacies studies

During the fieldwork, coherent volcanic facies were classified according to McPhie et al. (1993) and pyroclastic facies according to the criteria of Branney and Kokelaar (2002). These two classification methods are important in the field of volcanic geology, as they help to understand and categorize the different types of volcanic material, which in turn provides

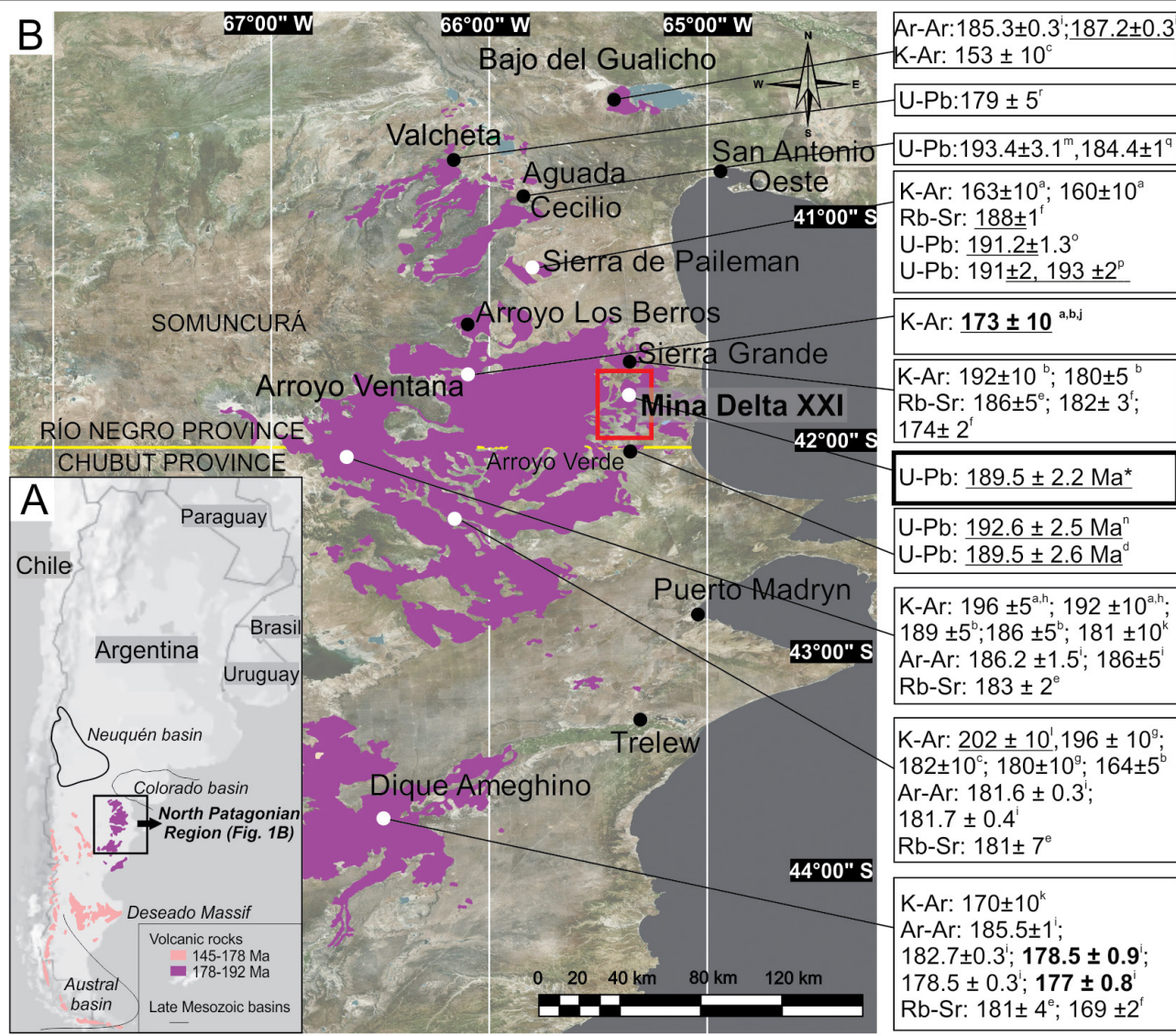


Figure 1. A. Southern South America map showing the distribution of Jurassic igneous rocks of Marfil Complex in the Chon Aike Magmatic province that includes V0, V1, and V2, located southern in the Deseado Massif. For general reference, the sedimentary late Mesozoic petroleum basins are indicated. B. Regional map showing the outcrops of the Marfil Complex in the northeastern Patagonia region. In the red square, the studied Mina Delta XXI area of Figure 2. In the margins, known and new radiometric ages for each location. References in the image are: a: Núñez et al. (1975); b: Cortés (1981); c: Lizuáin (1983); d: Pavón Pivetta et al. (2024); e: Rapela and Pankhurst (1993); f: Pankhurst and Rapela (1995); g: Page (1987); h: Busteros et al. (1998); i: Féraud et al. (1999); j: Franchi et al. (2001); k: Linares (1977); l: Yllañez (1979); m: Strazzere et al. (2019); n: Pavón Pivetta et al. (2020); o: Strazzere et al. (2022); p: Pugliese et al. 2021, q: González et al. 2022, r: Chernicoff et al. 2017 * This publication. Map simplified from Busteros et al. (1998); Caminos (2001); Franchi et al. (2001), González et al. (2013, 2017b and 2022), Pavón Pivetta et al. (2020) and Navarrete et al. (2024).

information about the eruptive processes and environmental conditions at the time of the eruption. Sedimentary facies were classified according to Miall (2006), which provides the background of the sedimentary environmental conditions that are critical for the development and preservation of the flora. Since the described deposit differs from conventional two-component lacustrine mixed sediments, we adopted the framework of a three-component mixing system (siliciclastic, volcanoclastic, and carbonates) proposed for lacustrine sedimentary systems by Wei et al. (2022). The carbonate rocks were described according to Dunham (1962), while abbreviations followed Whitney and Evans (2010).

The collected samples were examined using a Leica MZ95 stereomicroscope. Specific sectors of the samples were selected to make thin petrographic sections at the Laboratorio de Petrotomía of the Departamento de Geología- INGEOSUR, Universidad Nacional del Sur, and CONICET. These sections were analyzed using a Leica DM750P petrographic microscope.

U-Pb dating

U-Pb geochronology of the zircons from Sample MD 1b was performed in two laboratories. The initial processing, including milling, sieving, and panning to concentrate the zircon grains, was carried out at the Laboratorio de Petrotomía of the Departamento de Geología -INGEOSUR, of the Universidad Nacional del Sur and CONICET. After hand-picking the zircons, mounts were prepared for several samples at the Laboratorio Multiusuário (MultiLab) of the Departamento de Geología Regional e Geotectónica, Rio de Janeiro State University (UERJ). The U-Pb dating was carried out at the MultiLab using the *in situ* laser ablation technique (LA-MC-ICPMS) as described by Geraldès et al. (2015) and Costa et al. (2017). Analyses were performed with a Teledyne Analyte G2 Excimer laser system coupled to a Thermo Scientific Neptune Plus MC-ICP-MS instrument. The patterns used for the analyses included 91500 and GJ01, and the blanks were measured before each series of 10 laser spots.

Paleobotany and palynology

The plant remains illustrated here were found in a small quarry, located three km north of Mina Delta XXI, within sedimentary and volcanogenic rocks of the Puesto Piris Formation, in the Marifil Complex. The samples were examined using a Schonfeld Optic stereomicroscope and photographed with a digital camera and a TopCam 9 MP. The specimens are deposited at the paleontological collection of the Museo Provincial "María Inés Koop" in Valcheta, Río Negro Province, under the catalog numbers 1835/P/24, 1836/P/24, 1837/P/24

and 1838/P/24.

A small portion of sample MD-1b was processed for palynological analyses at the Laboratorio de Palinología of the Instituto Geológico del Sur (INGEOSUR)- Universidad Nacional del Sur (UNS) using conventional techniques for the extraction of the palynological organic matter with hydrochloric and hydrofluoric acids, following Volkheimer and Melendi (1976) and Riding (2021). Oxidation with nitric acid was performed to clarify the palynological organic matter. The residue was mounted using UV-curable acrylate (Trabasil® NR2) media (Noetinger et al. 2017). Slides were examined using a Nikon Eclipse 50i transmitted light microscope, and the illustrated specimen was captured with a microscope digital camera AmScope MU Series 14.0 MP. Slides and the residue are housed in the INGEOSUR-Universidad Nacional del Sur, Bahía Blanca, Argentina, under catalog number UNSP-6845.

RESULTS

Lithofacies description of Marifil Complex in Mina Delta XXI

Volcano-sedimentary rocks of the Marifil Complex, predominantly occupying lower topographic elevations, are particularly exposed along seasonal creeks and small quarries used for internal road construction. A detailed facies analysis was performed along four transects in the Mina Delta XXI area (marked with continuous white lines in Fig. 2), recognizing ten different lithofacies grouped into three facies associations.

Lithofacies 1: Massive paraconglomerate (Fig 3 A-B) characterized by subangular to subrounded granite clasts (90%) reaching up to two m in diameter, and metamorphic basement clasts (10%) of up to 20 cm. The matrix consists of more than 20% of feldspar-rich sand clasts with 5% juvenile volcanic components (glass shards). This lithofacies forms the basal layer of the volcano-sedimentary succession, directly overlying weathered Permian granites.

Lithofacies 2: Massive, coarse-grained arkosic sandstone (Sm), composed of poorly sorted sub-angular and sub-prismatic clasts of feldspar, plagioclase and quartz clasts, together with small granite pebbles. The matrix shows sericite alteration, and the cement is not clearly identifiable. The strike and dip of these beds are N55°/10°NW (Fig. 3 C).

Lithofacies 3: volcanic, medium to fine-grained sandstone and siltstone, with dispersed terrestrial macrophyte-derived fragments and compression-impressions of fossil plants. This lithofacies exhibits horizontal stratification, with colors ranging from yellow to faint purple. It is partially interbedded with massive, brecciated, and bituminous limestones of facies 3, 4, 5,

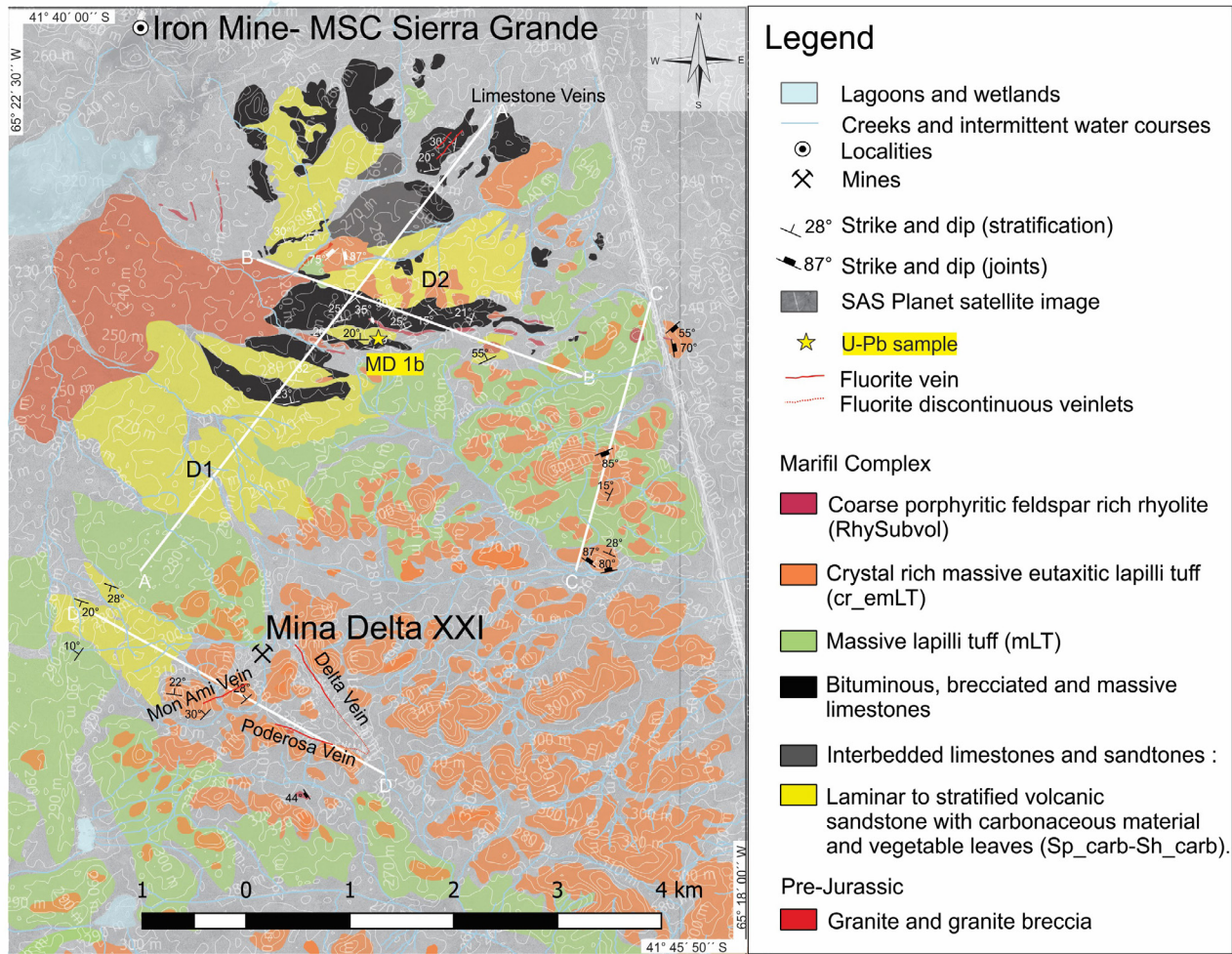


Figure 2. Detailed map of Mina Delta XXI indicating the outcropping facies, the location of the two depocenters (D1 and D2), the four transects (A-A' to D-D', white lines) from which the section of Figure 6 was logged. It also indicates the location of the fluorite mines and veins.

and 6. These layers are found in small quarries (Fig. 3 D) in the northern sector of Mina Delta XXI. The facies have a high proportion of juvenile components (shards). Clasts are angular, mainly of quartz, plagioclase and minor k-feldspars. The terrestrial macrophyte-derived fragments are carbonaceous, identified as dark, angular to irregular particles with distinct outlines (F1_carb).

The recovered plant remains are fragmented and incomplete, primarily preserved as impressions and representing both vegetative and reproductive parts of vascular plants. These remains include equisetalean stems attributed to *Equisetites* sp. (Fig. 4 A-C), leafy twigs identified as *Pagiophyllum* spp. (Fig. 4 E-F), a probable conifer pollen cone (Fig. 4 D), a probable bract/seed-scale complex (Fig. 4 H), and a leaf with prominent reticulate venation (Fig. 4 J-K) of uncertain affinity. Permineralized wood fragments (Fig. 4 G) were also found at two locations, approximately 400 m and two km south of the studied profile, although they were not collected from the field. Furthermore, one pollen grain assigned to *Inaperturopollenites indicus* Srivastava 1966 (Fig. 4 I) was recovered from one

palynologic sample.

Lithofacies 4: Mixed volcanic-clastic rock, terrigenous components consist of sand-sized and silt-sized particles (Sh). This facies consists of 2 to 3-cm thick tabular beds, composed of interbedded fine-grained sand and silts, composed of 45% terrigenous/clastic material, 35% volcanic components, and 20% carbonate. The terrigenous grains are subangular and have low sphericity. They are moderately selected and composed of feldspar, quartz, and scarce muscovite. Zircon was identified as an accessory. The matrix is 40% of the sample and comprises siltstone, with abundant volcanic material, feldspars, and quartz. The cement is formed by calcite, reacts with cold HCl (Fig. 5 A) and composes 20% of the sample. The depositional fabric is heterogeneous and planar, indicating textural segregation of the particles. Porosity is primary, intergranular, and moderate to good. Based on the classification proposed by Wei et al. (2022) this facies is classified as a mixed volcanic-clastic rock.

Lithofacies 5: Massive limestone (Lm_m). This lithofacies exhibits layering that ranges from centimeters to meters, form-

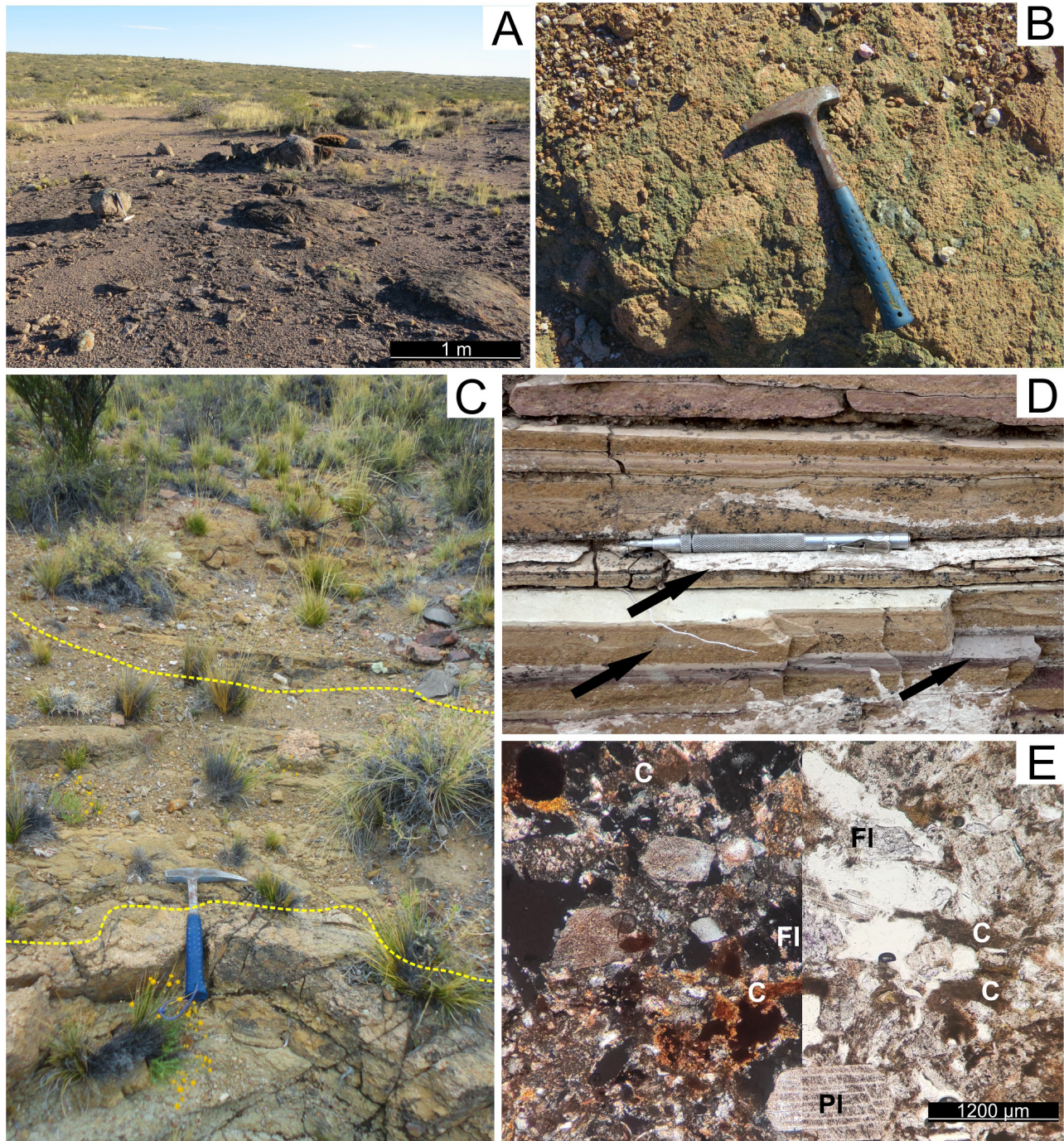


Figure 3. A-B. Massive paraconglomerate from Lithofacies 1, with a hammer for scale. A. General view of the outcrops. B. Detailed outcrop photograph showing angular to subrounded granite clasts in the matrix. C. Outcrops of the lithofacies 1, in the lower portion of the photograph, are covered discordantly by massive coarse-grained arkosic sandstone (Sm) of lithofacies 2 and lithofacies 3 (FI_{carb}) in the upper portion of the photograph. D. Black arrows indicate the *in situ* fossil leaf remains in small quarries of siltstone and limestone of lithofacies 3 in Mina Delta XXI. E. Lithofacies 3 microphotograph (left with cross-polarized light, right with parallel light), C= organic matter elongated perpendicular to the stratification plane, Pl= plagioclase and F= K-feldspars.

ing beds up to five m thick (Fig. 5 C-D). It is partially interbedded with Lithofacies 2. The outcrop appears grey to dark grey, with a coarse texture that becomes distinct on weathered stratified surfaces. According to Dunham (1962), the rocks composing this lithofacies was classified as wackestone. It contains over 10% grains, including 5% quartz, 3% feldspars,

1% muscovite, and 1% accessory minerals. In certain layers, rounded chert formations are situated adjacent to the brecciated limestones. Lithofacies 5 hosts a series of fluorite veins located northeast of the study area. Petrographic studies have identified scarce calcite near the vein walls, silica replacement, and kaolinite.

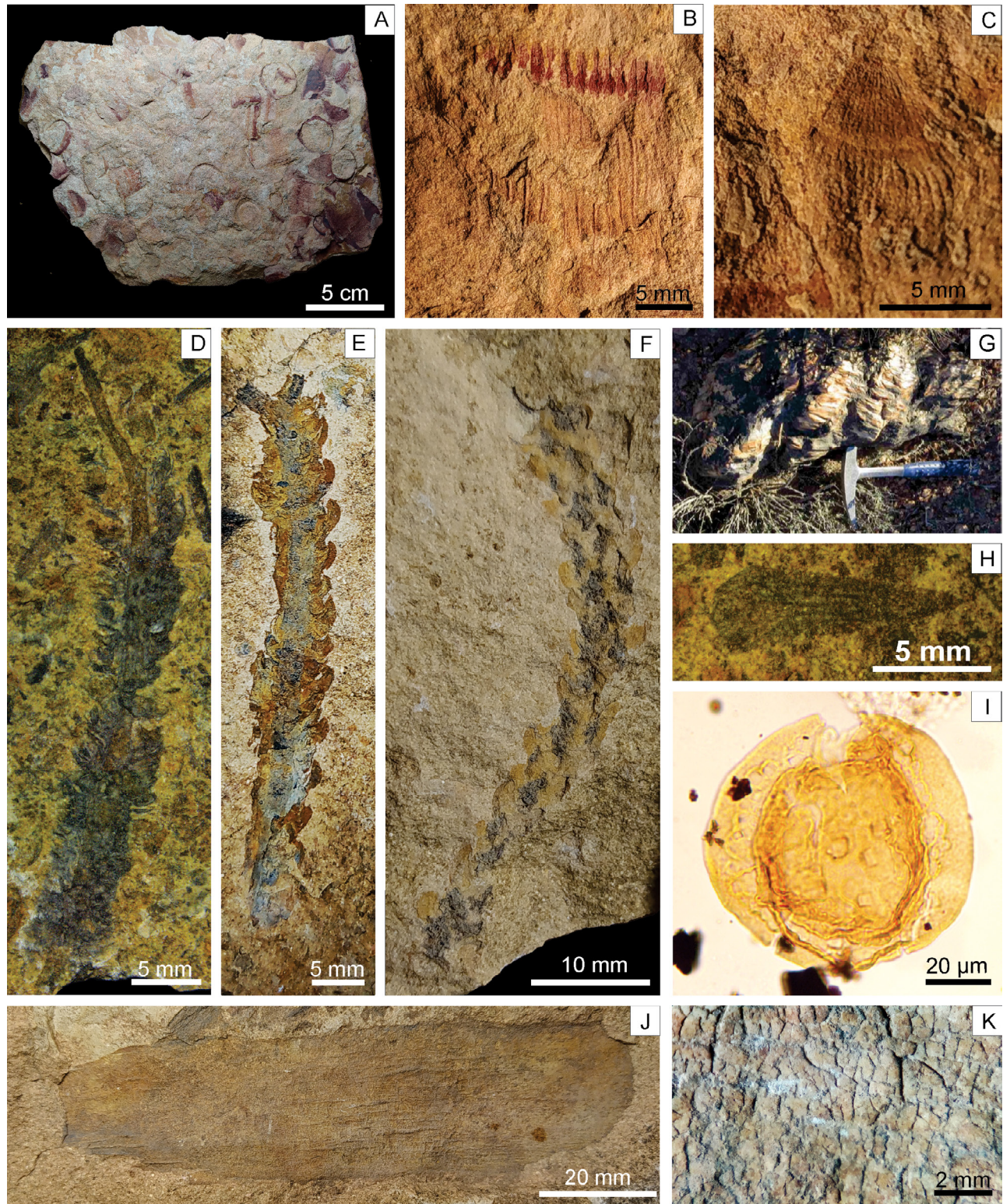


Figure 4. A-C. *Equisetites* sp. (1835/P/24). D. Probable conifer pollen cone. 1837/P/24. E-F. *Pagiophyllum* spp. 1838/P/24. G. Permineralized wood remains located near the studied section. H. Probable bract-scale complex (1837/P/24). I. *Inaperturopollenites indicus* Srivastava, 1966 (UNSP-6358-C; K25/1). J-K. Fragment of an indeterminate leaf with reticulate venation (1838/P/24). K. Detail of the reticulate venation in J.

Lithofacies 6: Brecciated limestone (Lm_{bx}). This facies is observed in the northern zone of Mina Delta XXI, where it is interbedded with extensive massive limestone (Fig. 5 D). The breccia texture is attributed to partial dissolution of

the limestone in localized sectors. The rock is composed of wackestone (Dunham (1962) clasts in a calcite cement, with no matrix present, and classified as a floatstone. The organic matter gives it a dark grey color and foul odor. In some outcrop

areas, chert silica infill is observed. In the northern part of the study area, this facies contains dark purple fluorite veins.

Lithofacies 7: Bituminous limestone (Lm_bit). The lithofacies is classified as boundstone and mudstone according to Dunham (1962), consisting of finely layered beds of these two types interbedded with lithofacies 3 and 4. When the beds

are fractured, a distinct foul odor is released. The stratification in these beds is the result of microbial processes, which lead to synchronous precipitation of carbonates and the accumulation of organic matter. Notably, stromatolites have been recognized within specific strata (Fig. 5 E), further indicating microbial influence on the carbonate precipitation. Evidence of

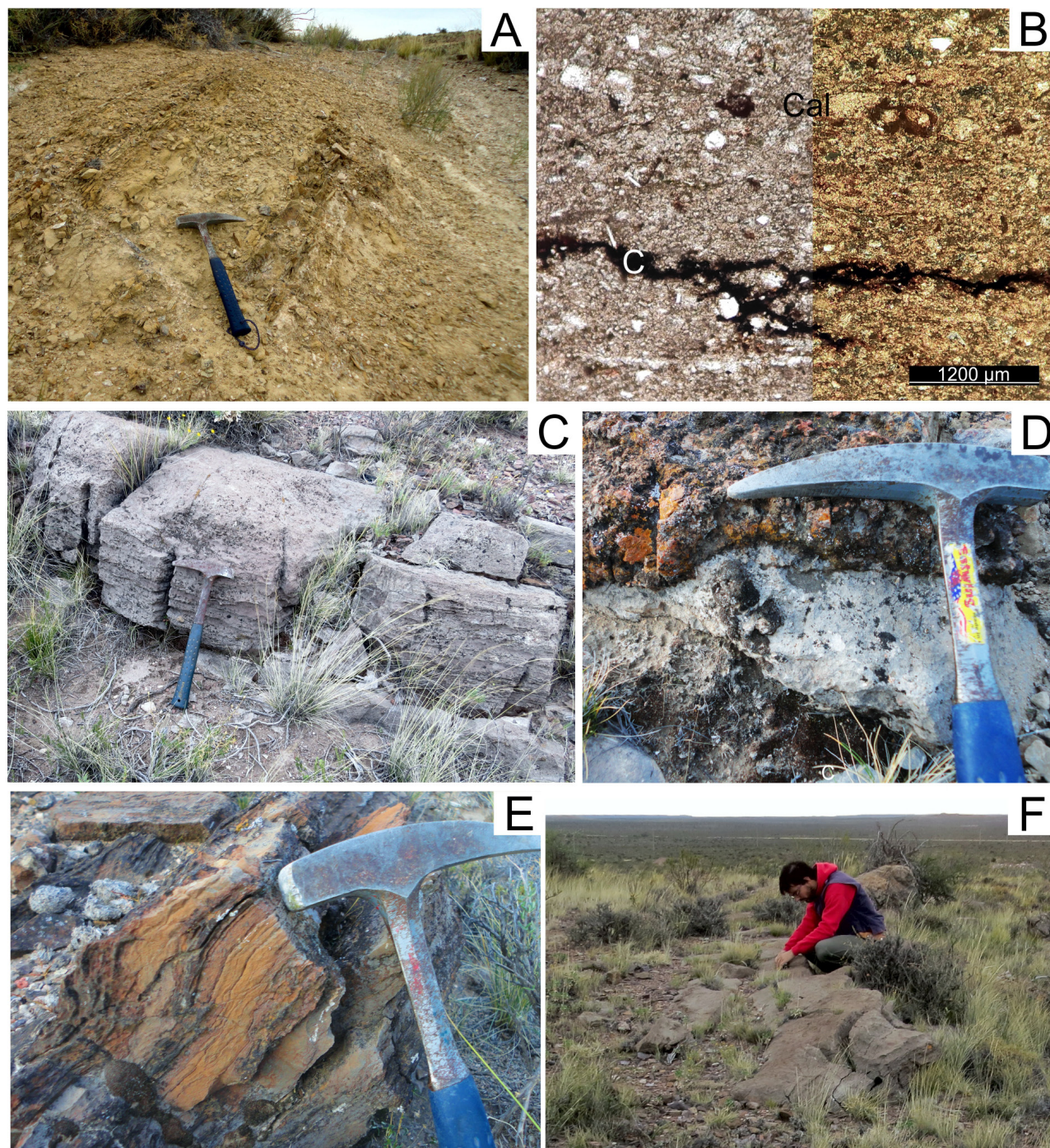


Figure 5. A. Mixed volcanic-clastic rock, in an outcrop of Lithofacies 4 (hammer for scale). B. Microphotograph, to the left with parallel light and right with crossed Nicols. Cal= calcite, C= coal, organic material. C. Massive limestone outcrop of lithofacies 5 (with a hammer for scale) showing erosion marks and incipient bedding. D. Massive limestone (Lm_m) covered by brecciated limestone (Lm_bx) of lithofacies 6. E. bituminous limestone with stromatolites (Lm_bit). F. Field photograph of lithofacies 4 outcrops (Sh) assigned as mixed volcanic-clastic rock (Wei et al. 2022) where terrigenous components are sand and silt-sized.

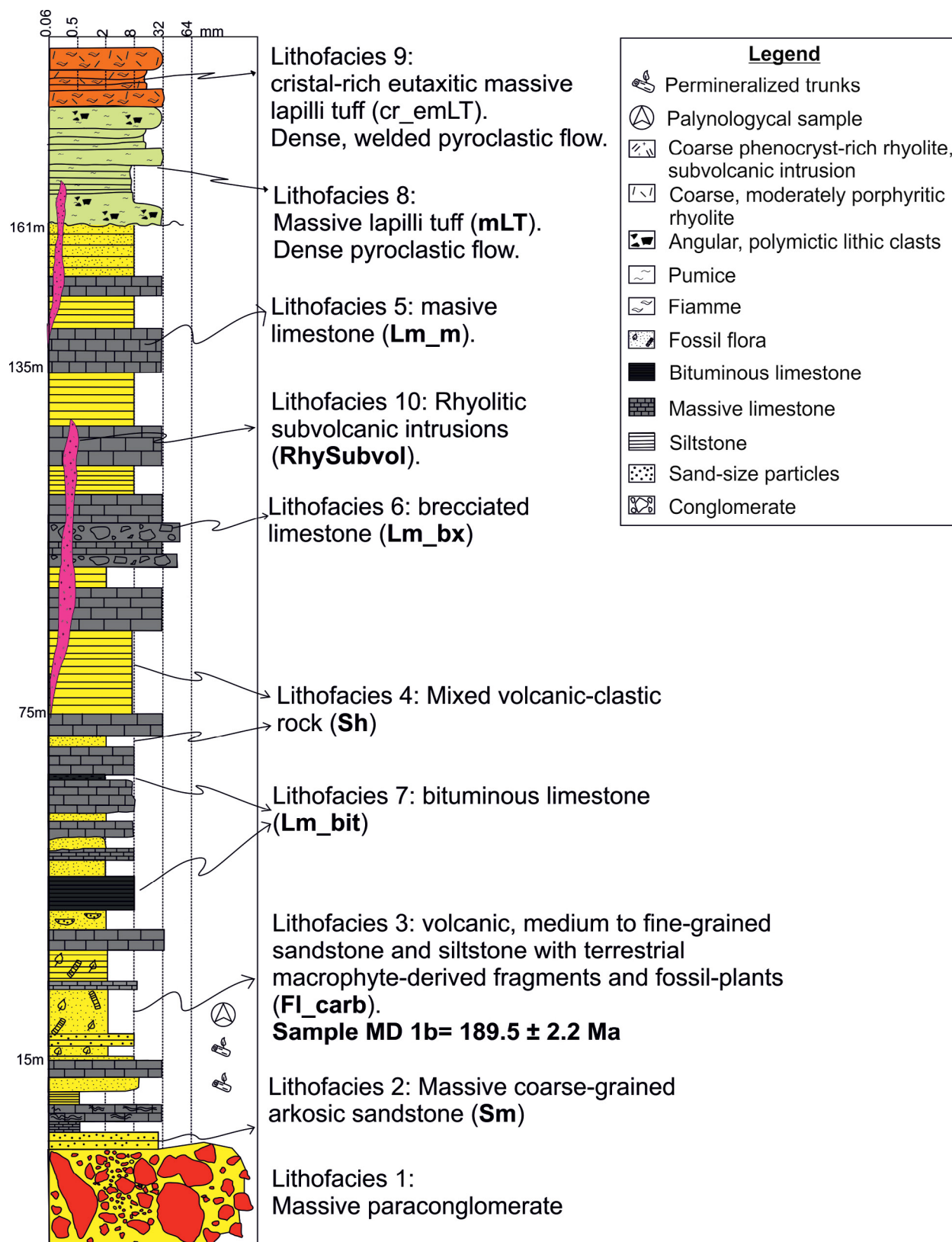


Figure 6. Stratigraphic section based on outcrop transects performed in the Mina Delta XXI area. The micro and macrofossils recovered in this study are indicated in the lithological section.

bioturbation is evident in the stratification planes. The above-mentioned lithofacies are located in the stratigraphic column

where interbedding of the lithofacies 1 to 7 is clear (Figure 6).
Lithofacies 8: massive lapilli tuffs (mLT). This lithofacies

is located in erosive contacts, especially the volcano-sedimentary (lithofacies 1 to 7). At Mina Delta XXI, this lithofacies consists of a 100 m thick succession of acidic massive lapilli tuffs composed of a flow supported by a rhyolitic matrix with angular basement lithic clasts (Fig. 7 B). The base is erosive and is moderately welded, always located beneath the highly welded erosion-resistant lithofacies 9 (Fig. 7 A). The outcrops described are located in creeks and consist of a massive lapilli tuff with pebble-sized lithic fragments (4–64 mm), where 10% are subangular metamorphic and 5% subrounded granitic. Ten percent of the sample has flattened pumice fragments and 20% quartz crystalloclasts up to five mm long. Both the matrix and pumice fragments are altered to clays, the matrix shows flow alignment around the lithic fragments.

Lithofacies 9: The crystal-rich eutaxitic massive lapilli tuff (cr_emLT) represents the most developed facies in the Mina Delta XXI area. It shows a higher welding degree, with eutaxitic textures (Fig 7 C). Under the microscope, the rock displays up to 10% rhyolitic fragments, 15% crystalloclasts, formed of quartz and potassic feldspar. The matrix constitutes 30% of the rock and develops a rheomorphic flow around the quartz crystalloclasts that show brittle fractures and reabsorption embayments similar to the description of Pavón Pivetta et al. (2020).

This lithofacies occupies a substantial portion of the south-

eastern sector of the Mina Delta XXI area and embodies some of the most distinctive features of the Marifil Complex. It is interpreted as the welded equivalent of the massive lapilli tuffs of lithofacies 8. Eutaxitic lapilli tuff is the most common lithofacies in ignimbrite deposits and it is considered that it was generated by the collapse of sustained high-temperature pyroclastic plumes (Branney and Kokelaar 2002).

Lithofacies 10: This lithofacies consists of porphyritic, rhyolitic rocks that intrude all the previously described facies (RhySubvol). The contact between this lithofacies and the previously described ones is sharp, with a small reaction rim (Fig. 7 D-E). This reaction rim is sometimes only observable in thin sections under a microscope. It is considered as the youngest lithofacies of the Marifil Complex in this area. The texture is porphyritic with quartz phenocrysts up to five mm and sanidine up to one cm located in a finer groundmass with the same composition. Quartz is found as glomeruli of different sizes. Sanidine phenocrysts have albite rims (Fig. 7 F-G).

Lithofacies associations

Three lithofacies associations were differentiated. Lithofacies 1, 2, 3 and 4 (Sm, FI_carb, and Sh) represent lithofacies association 1 (FA 1), interpreted as braided stream deposits in alluvial fans (Sm), followed by overbank or waning deposits (FI_carb). They were probably deposited in small fault-bound-

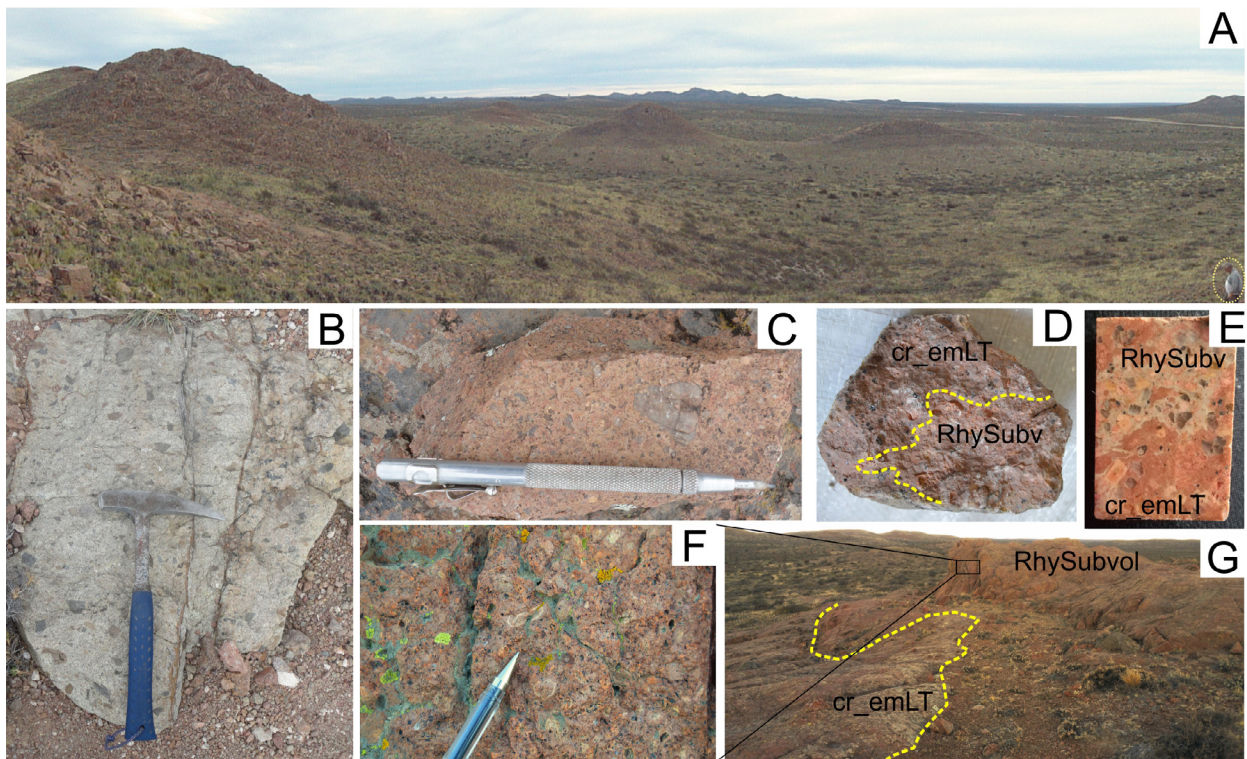


Figure 7. A. Landscape view of lithofacies 8 and 9 towards the north. B. Lithofacies 8 outcrop, with a hammer for scale. C. Hand specimen of lithofacies 9 (cr_emLT). D. Hand specimen of lithofacies 9 and 10. E. Contact between cr_emLT and RhySubvol. F. Detail of outcrop of facies 10. G. Lithofacies 10 outcrop.

ed grabens; however, a detailed architectural characterization of the sedimentary banks is needed to further support these interpretations. FA 1 is situated in two different sectors: the first is elongated in an N290°W direction, located to the south of a granitic topographic high (D1, Fig. 2), while the second is found to the north of this granite topographic high and extends in an E-W direction (D2, Fig. 2).

FA 2 comprises lithofacies 4, 5, and 6. This FA reflects very low energy conditions during sediment deposition. Fine-grained sandstone lenses and tabular limestone banks are interpreted as forming the deeper deposits of a lacustrine environment. Bioturbation and stromatolites are common in the stratification planes of some limestone beds, together with deeply sculptured, elephant-skin-like surfaces, indicative of

subaerial exposure and erosion. This facies association is interpreted as low-energy deposits within the continental basin.

Field observations and subsequent mapping (Fig. 2) clearly show that the volcano-sedimentary facies are confined to the northern part of the Mina Delta XXI area. In the field, FA 1 and FA 2 cover the Permian granite in erosional unconformity and the Sierra Grande Formation in angular unconformity. Although the Sierra Grande Formation is not exposed within the mapped area, it has been identified two km to the north, near the Sierra Grande Iron Mine.

FA 3 comprises lithofacies 8, 9, and 10. This FA is completely separated from the previous ones by an erosional unconformity. Volcanism of this FA was defined 20 km south on the border of the provinces of Rio Negro and Chubut by

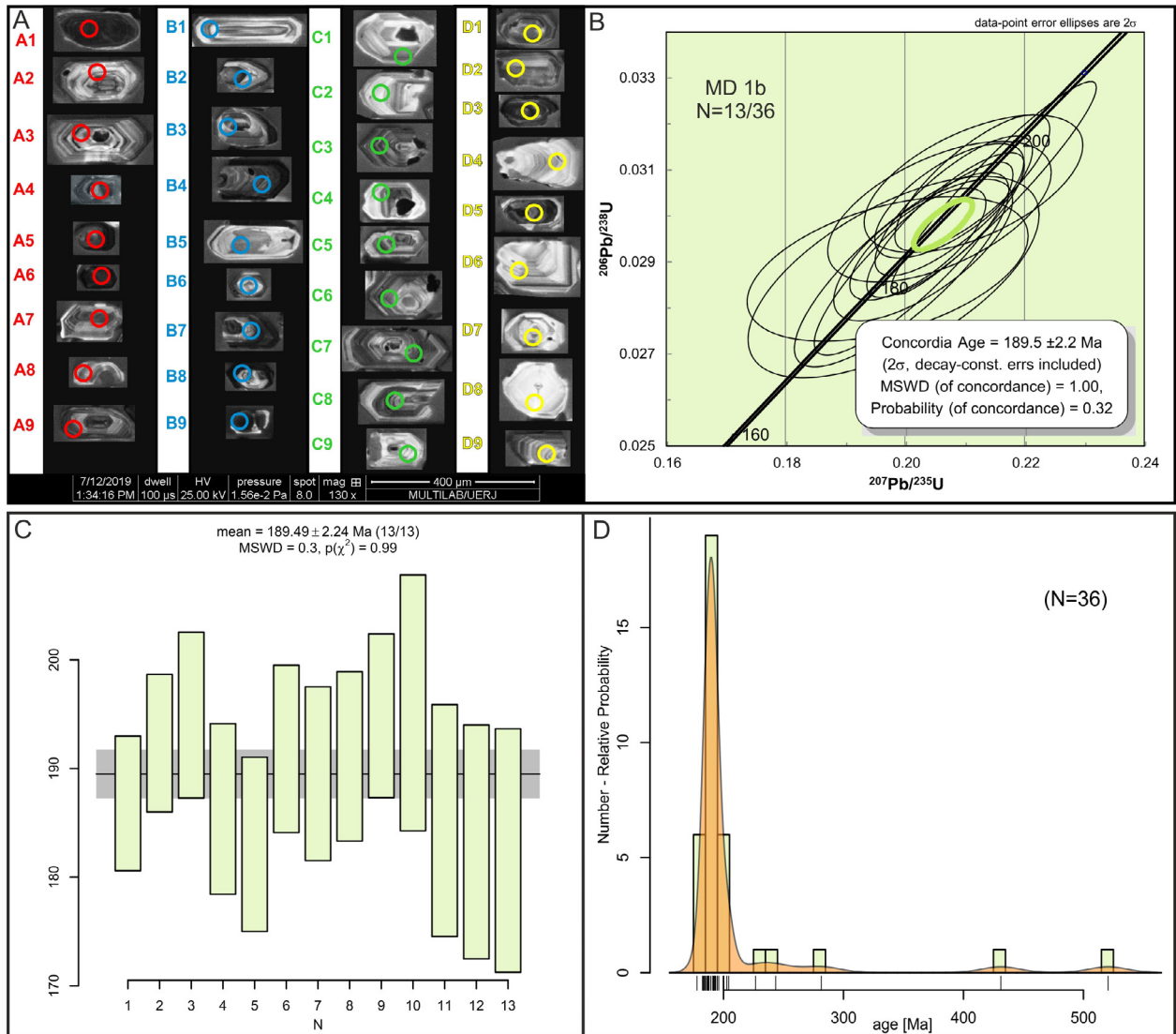


Figure 8. A. SEM cathodoluminescence image of zircon grains belonging to sample MD 1b showing euhedral, clear magmatic origin. The position of laser spots is indicated in circles. B. $^{206}\text{Pb}/^{238}\text{U}$ versus $^{207}\text{Pb}/^{235}\text{U}$ diagram showing the Concordia curve and Concordia age. C. Probability plot of sample MD 1b with the best age of $189.49 \pm 2.24 \text{ Ma}$. D. Probability density plot showing the $^{238}\text{U}/^{206}\text{Pb}$ age distribution of the youngest and most abundant populations of the analyzed crystals. It is evident there is a unimodal distribution of the 36 analyses and the oldest ages evidenced in the histogram are due to inherited zircon cores. Because of this, we interpret a nearly magmatic age for lithofacies 3.

Pavón Pivetta et al. (2020). These authors interpreted this FA as another volcanic event, with a particular geochemical characteristic and a geochronological range that varies between 188-178 Ma and is assigned to V1. FA 3 covers all the volcano-sedimentary lithofacies and allows their preservation in the Mina Delta XXI area.

New geochronological data

To determine the depositional age of the Puesto Piris Formation and the eruptive age of the first facies of the Marifil Complex, we analyzed the zircons from sample MD 1b, which is the same sample that contains macro- and microflora remains.

Thirty-six zircons were analyzed in this sample (Table 1, Fig. 8 A): eight with low U values (<100 ppm), 20 with intermediate concentrations (100 – 300 ppm), and eight with high U concentrations (300 – 807 ppm). The Th/U ratios are elevated (>0.5 ppm with an average of 1.22 ppm, minimum 0.64 and 2.51 ppm), indicating a magmatic origin (Rubatto 2002).

Thirteen analyses were used to build a Concordia curve, yielding an age of 189.5 ± 2.2 Ma (MSWD=1.00) with a concordance probability of 0.32 (Fig. 8 B). This early Pliensbachian age (Cohen et al. 2013: updated) is interpreted as the crystallization age of the volcanic components of lithofacies 3. The relative probability diagram (Fig. 8 C) includes the same 13 zircons, which are also plotted on the Concordia diagram, showing a median age of 189.49 ± 2.24 Ma with a mean square weighted deviation (MSWD) of 0.3.

Four analyses were excluded due to isotopic deviation of $^{207}\text{U}/^{236}\text{U}$ (sigma error > 45%), and five analyses were excluded for concordance percentages between 8 and 14%. One zircon, indicating an age of 520 Ma, was identified as a core without inclusions but it displayed a marked discontinuity at the rim, suggesting an inherited origin; this zircon was also excluded from the Concordia diagram. A similar case was observed with a zircon dated at 432 Ma age (Silurian- Wenlock), further indicating that the unit may have assimilated older Cambrian and Siluro-Devonian basement zircons (Fig. 8 D). Additionally, two zircons, dated at 281 Ma and 247 Ma, were attributed to the underlying Permian granites and were also discarded, as they were probably assimilated during volcanic ascent.

DISCUSSION

Paleoenvironmental reconstruction of the Early Jurassic of Northern Patagonia.

Stratigraphic analyses, supported by isotopic dating and paleobotanical and palynological data, enabled the recon-

struction of the early Pliensbachian environment, interpreted as a small lacustrine continental basin adjacent to an explosive volcanic center. Equisetalean plants grew near the water body, while gymnosperm vegetation dominated the surrounding area of the basin.

Facies Associations 1 and 2 represent a continental basin, transitioning from alluvial fans, braided fluvial to lacustrine conditions, where sandstones and limestones accumulate or precipitate in topographic lows. Scarce transportation of the clasts from their origin is interpreted for FA 1. Compositional mixing in FA 1 and FA 2 is generally attributed to depositional processes that are active during sedimentation, where siliclastic and carbonate particles became intermixed during sediment accumulation (Chiarella et al. 2017). This accumulation occurs either because these particles constitute the majority of the transported sediment at the same time or because the continuous supply of terrigenous particles does not significantly inhibit *in situ* carbonate production (Chiarella et al. 2009, 2016; Chiarella 2011; Longhitano et al. 2012).

Deposition is primarily controlled by gravitational flows at the base, although they are not well preserved in the Mina Delta XXI sector. This is followed by low-energy lacustrine sedimentation and coetaneous juvenile-bearing volcanic sediments.

The presence of chert within the limestones suggests that diagenesis played a role in altering the original limestone, leading to partial chertification, a process observed in Phanerozoic carbonates, carbonate-bearing sandstones, evaporites, and fossil wood (Hesse 1989). This author proposed that the source of silica can be distinguished based on the extent of chertification, with partial chertification indicating a biogenic origin and pervasive chertification suggesting an inorganic source. In the Mina Delta XXI area, partial chertification, occurring near leaf imprint levels and permineralized wood remains, suggests that the silica source may be predominantly biogenic, probably formed in an anoxic environment. In carbonates and carbonate-bearing sandstones, silica is introduced both through pore-filling cementation and the replacement of carbonate by silica (Hesse 1989). Further north, pervasive to complete silicification is observed near the fluorite-bearing veins (limestones veins, Fig. 2), indicating that the silica source is predominantly inorganic (Hesse 1989), probably associated with hydrothermal-volcanogenic rocks.

Facies Association 2 is interpreted as representing very low-energy sediment deposition, characterized by tabular banks of fine-grained sandstones, muds, and limestones, typical of offshore sedimentary deposits in a lacustrine environment system. Bioturbation, burrow marks, and bioclastic fossils are commonly observed on the stratification planes

Table 1. "in situ" U-Pb data in zircon grains, obtained by LA-MC-ICPMS for sample MD 1b. The first 13 data were used for the Concordia curve.

Spot number	f 206a	Pb ppm	Th ppm	U ppm	Th/Ub	207Pb/235U [%]	1 s 206Pb/238U [%]	1 s 206Pb/238U [%]	Rhod	207Pb/206Pbe [%]	1 s 206Pb/238U [%]	206Pb/238U	1 s 207Pb/235U abs	207Pb/206Pb	1 s abs	% Concf			
MD 1b (B)2	0.0077	11	355	263	1.35	0.2019	4.61	0.0294	3.38	0.73	0.0498	3.13	187	6	187	9	187	6	100
MD 1b (B) 3	0.0098	7	237	148	1.60	0.2072	4.92	0.0303	3.35	0.68	0.0495	3.60	193	6	191	9	173	6	111
MD 1b (B) 6	0.0371	3	107	70	1.52	0.2112	7.08	0.0307	3.98	0.56	0.0499	5.85	195	8	195	14	190	11	102
MD 1b (C) 1	0.0249	5	175	104	1.68	0.2028	6.03	0.0293	4.29	0.71	0.0503	4.24	186	8	187	11	207	9	90
MD 1b (C) 2	0.0384	2	67	60	1.11	0.1968	9.76	0.0288	4.45	0.46	0.0495	8.69	183	8	182	18	171	15	107
MD 1b (C) 3	0.0085	12	393	259	1.52	0.2079	5.18	0.0302	4.10	0.79	0.0499	3.16	192	8	192	10	190	6	101
MD 1b (C) 4	0.0108	11	260	278	0.94	0.2065	5.21	0.0298	4.31	0.83	0.0503	2.93	189	8	191	10	207	6	91
MD 1b (C) 7	0.0140	7	194	172	1.13	0.2055	7.44	0.0301	4.15	0.56	0.0495	6.17	191	8	190	14	173	11	110
MD 1b (C) 8	0.0182	6	186	127	1.47	0.2110	5.02	0.0307	3.95	0.79	0.0498	3.10	195	8	194	10	186	6	105
MD 1b (D) 2	0.1017	11	345	250	1.38	0.2146	6.55	0.0306	6.19	0.94	0.0509	2.15	194	12	197	13	234	5	83
MD 1b (D) 6	0.0298	4	141	86	1.64	0.2012	6.75	0.0291	5.89	0.87	0.0502	3.30	185	11	186	13	204	7	91
MD 1b (D) 7	0.0270	4	153	95	1.60	0.1992	7.36	0.0288	5.99	0.81	0.0501	4.29	183	11	184	14	200	9	92
MD 1b (D) 8	0.0745	2	46	39	1.20	0.1978	10.06	0.0287	6.24	0.62	0.0500	7.89	182	11	183	18	197	16	93
MD 1b (C) 6	0.0197	5	152	114	1.34	0.2005	5.90	0.0295	4.44	0.75	0.0493	3.89	187	8	186	11	162	6	115
MD 1b (B) 7	0.0045	12	273	294	0.93	0.2074	3.82	0.0305	3.29	0.86	0.0494	1.94	194	6	191	7	165	3	117
MD 1b (D) 9	0.0233	5	141	119	1.18	0.2056	7.56	0.0298	5.78	0.76	0.0500	4.87	189	11	190	14	196	10	97
MD 1b (D) 5	0.0093	11	298	249	1.20	0.2124	6.09	0.0303	5.59	0.92	0.0509	2.42	192	11	196	12	234	6	82
MD 1b (A) 1	0.0330	22	474	519	0.91	0.2560	5.10	0.0317	3.44	0.67	0.0586	3.77	201	7	231	12	552	21	36
MD 1b (A) 2	0.0819	9	322	155	2.07	0.4140	8.70	0.0306	3.81	0.44	0.0983	7.82	194	7	352	31	1591	124	12
MD 1b (A) 3	0.1067	7	169	130	1.30	0.4878	45.43	0.0303	6.38	0.14	0.1168	44.98	192	12	403	183	1908	858	10
MD 1b (A) 5	0.1302	41	626	807	0.78	0.7241	51.99	0.0376	17.76	0.34	0.1395	48.86	238	42	553	288	2221	1085	11
MD 1b (A) 6	0.0737	28	593	745	0.80	0.4158	61.84	0.0322	12.35	0.20	0.0935	60.59	205	25	353	218	1498	908	14
MD 1b (A) 8	0.2987	8	142	161	0.88	0.7621	116.98	0.0324	13.20	0.11	0.1705	116.23	206	27	575	673	2563	2979	8
MD 1b (A) 9	0.0247	8	207	192	1.08	0.2337	7.86	0.0303	3.53	0.45	0.0559	7.02	193	7	213	17	447	31	43
MD 1b (B) 1	0.0303	4	153	61	2.51	0.2444	6.58	0.0316	3.51	0.53	0.0562	5.57	200	7	222	15	459	26	44
MD 1b (B) 8	0.0991	38	586	797	0.74	0.5794	7.15	0.0330	4.14	0.58	0.1274	5.83	209	9	464	33	2063	120	10
MD 1b (B) 4	0.0051	14	168	262	0.64	0.3231	3.84	0.0446	2.45	0.64	0.0525	2.95	281	7	284	11	309	9	91
MD 1b (B) 5	0.0075	7	62	79	0.78	0.5134	3.59	0.0694	1.99	0.56	0.0537	2.98	432	9	421	15	358	11	121
MD 1b (C) 9	0.0086	19	297	417	0.71	0.2712	8.08	0.0390	7.65	0.95	0.0505	2.60	247	19	244	20	216	6	114
MD 1b (D) 3	0.0028	39	268	365	0.73	0.6700	3.01	0.0841	2.29	0.76	0.0578	1.96	520	12	521	16	522	10	100
MD 1b (C) 5	0.0311	9	176	209	0.85	0.2468	8.61	0.0303	4.00	0.46	0.0591	7.63	192	8	224	19	571	44	34
MD 1b (B) 9	0.0389	16	357	409	0.87	0.2234	5.21	0.0297	4.46	0.86	0.0545	2.68	189	8	205	11	392	11	48
MD 1b (A) 4	0.0152	28	866	618	1.40	0.2247	5.05	0.0315	3.68	0.73	0.0518	3.46	200	7	206	10	275	10	73
MD 1b (A) 7	0.0223	9	337	201	1.68	0.2050	7.79	0.0289	3.86	0.49	0.0515	6.77	184	7	189	15	261	18	70
MD 1b (D) 1	0.0110	10	325	231	1.41	0.2107	6.57	0.0294	5.78	0.88	0.0519	3.12	187	11	194	13	283	9	66
MD 1b (D) 4	0.0213	4	122	98	1.25	0.2073	6.67	0.0293	5.85	0.88	0.0512	3.19	186	11	191	13	251	8	74

of these beds. This description agrees with Strazzere et al. (2019) in the Puesto Piris area, where they also reported thin layers of volcanic ash, approximately 10 cm thick, interbedded within the limestone facies. Zanettini (1981) suggested that the finer sediments, such as siltstones, represent flood-plain deposits with density currents, while the interbedded limestones indicate lacustrine conditions during a more stable tectonic period.

Facies Association 3 is interpreted in this study as representative of an explosive volcanic event that ended all the pre-existing flora development, covering the landscape with a hundred or more meters of rhyolitic pyroclastic rocks. This facies association is interpreted as ignimbrites located laterally to the volcanic vent and represents a high explosive eruptive stage (Cas and Wright 1987). This association is similar to and can be correlated with the massive lapilli tuff described in Pavón Pivetta et al. (2020), located 20 km to the south. These catastrophic explosions may be related to some type of caldera event, involving large volume pyroclastic flows, although further data must be processed to confirm this possibility.

Micro and macrofloral record of the Puesto Piris Formation and comparisons with other Early Jurassic floras of Patagonia

To date, the presence of plant fossils within the epiclastic and volcanoclastic facies associated with the Marifil Complex has been relatively little studied. The earliest known reference can be found in Nuñez et al. (1975), who identified the existence of at least four fossiliferous sedimentary levels in the Marifil Complex. They reported the presence of leaves of the genera *Otozamites*, *Dictyozamites*, and *Ptilophyllum*. Díaz-Martínez et al. (2017) also mentioned the presence of fossil plants attributed to equisetaleans, found in sedimentary levels associated with Early Jurassic volcanism, a few meters above a level of dinosaur footprints. Strazzere et al. (2019) reported the presence of stromatolites and an incomplete equisetalean stem preserved as an impression from limestones located 20 km SE of Valcheta and 100 km north of the study area. A colony of the algae *Botryococcus* was also illustrated from palynologic samples from the same levels. The age of this association was restricted to the Sinemurian based on a 193.4 ± 3.1 Ma zircon U/Pb age obtained from interbedded lava flows of the Marifil Complex. Other plant fossil remains found in the area correspond to the axis of a tree fern stem and wood remains referred to as '*Araucarites*' (*Agathoxylon*), all preserved as charcoalified fragments in conglomerate levels (Strazzere et al. 2019).

The fossils reported here add to the paleobotanic record of the Puesto Piris Formation, part of the Marifil Complex, in-

corporating equisetalean stems identified as *Equisetites* sp., as well as vegetative and reproductive structures of conifers -*Pagiophyllum* spp., a probable bract/seed-scale complex and a pollen cone-, together with an incomplete fragment of a leaf with reticulate venation of uncertain affinity.

One gymnosperm pollen grain assigned to *Inaperturopollenites indicus* Srivastava (1966) (Fig. 5 I) was recovered in palynologic samples from the same stratigraphic levels. This species is known from the Upper Triassic Chihuido Formation in the Malargüe Depocenter (Volkheimer and Papú, 1993), and the Upper Triassic Potrerillos Formation in the Cacheuta Basin (Zavattieri 1986, 1987 in Volkheimer and Papú, 1993). In the Neuquén Basin, this species was reported from the Lower Jurassic Piedra Pintada Formation (Arguijo and Volkheimer, 1985, in Volkheimer and Papú, 1993), mainly from Lower and Middle Jurassic (Volkheimer, 1968, 1969, 1971 and 1972; Martínez et al. 2001, 2005) and Lower Jurassic units (Olivera et al. 2010). It is also present in the Aalenian of the Cañadón Asfalto Basin (Olivera, 2015).

The paleoflora of the Piedra Pintada Formation also shows low diversity, as occurs in the Puesto Piris Formation, with almost half of the taxa in this unit being exclusive to the Lower Jurassic or Triassic. An Early Jurassic age for the Piedra Pintada Formation was first suggested based on ammonites and plant fossils (Ferello 1947; Herbst 1966). More recently, SHRIMP U-Pb isotopic dating of zircons from a tuff provided a magmatic crystallization age of 191.7 ± 2.8 Ma, confirming a Sinemurian-Pliensbachian age for the formation (Spalletti et al. 2010).

The plant association of the Piedra Pintada Formation has been compared with the highly diverse and abundant taphoflora from the neighboring Nestares Formation, whose age was originally interpreted as Hettangian based on its megafloora (Arrondo and Petriella, 1980), and later as Sinemurian based on new paleofloristic information and stratigraphic correlations with the isotopically dated Piedra del Águila Formation, or late Toarcian as inferred by the palynological content of samples from the upper levels of the unit (Zavattieri and Volkheimer 2003; Zavattieri et al. 2008; see also Gnaedinger and Zavattieri 2017).

A comparison of the Puesto Piris Formation taphoflora with those from other Early Jurassic units, from the provinces of Neuquén (e.g. El Freno, Piedra del Águila formations) and Chubut (Cañadón del Zaino, Cerro Bayo and Cerro Moschio localities) and the Antarctic (Hope Bay and Botany Bay), is difficult due to its low diversity, abundance, and poor preservation. The absence of index macrofossils in the Puesto Piris Formation makes it challenging to assign a precise age solely based on its flora. However, similarities with low-diversity as-

sociations in other Sinemurian- Pliensbachian units, such as the Piedra Pintada Formation, provide a tentative framework for comparison.

In this context, radiometric dating offers a robust and independent constraint on the age of the Puesto Piris Formation. The U/Pb (LA-ICPMS laser ablation) Concordia age of 189.5 ± 2.2 Ma reported here confirms an early Pliensbachian age. This radiometric evidence complements the paleofloristic interpretations and highlights the value of integrating multiple lines of evidence. Furthermore, radiometric dating constitutes an essential age proxy that helps to constrain and solve some disagreements regarding the ages of certain units as well as to reconstruct the paleofloristic evolution of Patagonia during the Early Jurassic.

The age of the Marifil Complex along the eastern North Patagonia region.

Figure 1 synthesizes the isotopic ages of Northern Patagonia indicating an Early and Middle Jurassic and providing a comprehensive overview of the region.

The age of 189.6 ± 2.5 Ma described for Lithofacies 3 is comparable to the U-Pb age of 193.4 ± 3.1 Ma reported by Strazzere et al. (2019) for a trachytic lava flow in Aguada Cecilio. It is also similar to the Concordia age of 191.2 ± 1.3 Ma for subvolcanic domes in the Sierra de Pailemán (Strazzere et al. 2022). In addition, this age is consistent with the 191 ± 2 and 193 ± 2 Ma ages reported by Pugliese et al. (2021) for rocks located 80 km to the north, in the Mina Gonzalito area. The Concordia age of 192.6 ± 2.5 Ma was obtained in a *coulée* at Arroyo Verde (Pavón Pivetta et al. 2020) and 189.5 ± 2.6 Ma in a dacitic lava flow (Pavón Pivetta et al. 2024). Towards the south, in the Dique Ameghino area, the Ar-Ar age of 185.5 ± 1 and 182.7 ± 0.3 (Féraud et al. 1999) suggests that the V0 event may continue. Navarro et al. (2015) dated the Grupo Chubut in the Telsen area, with detritic U-Pb age in zircons and they observed an inherited grain population with a range of 189 to 181 Ma that they assigned to the Marifil Complex. These authors indicated that the detrital zircon population is predominantly Jurassic, implicating the Marifil Formation as the nearby input source of provenance in both analyzed samples.

All these radiometric ages, and the one provided here, continue to emphasize the existence of a previous volcanic event named V0 (Pavón Pivetta et al. 2020) and evidenced by the possible presence of a flat slab break-off produced at the same age (Navarrete et al. 2019 a and b, Gianni et al. 2018, 2019 and 2023). The importance of these ages, together with paleontological data, is crucial to delineate the age and environment of the Lower Jurassic, mainly to determine the exten-

sion of this volcanism and its association with low sulfidation epithermal deposits (Pavón Pivetta et al. 2024).

CONCLUSIONS

The Marifil Complex in the Mina Delta area shows a good development of volcano-sedimentary facies, including matrix-supported breccias, arkosic sandstones, calcareous sandstones and siltstones, massive limestones, brecciated limestones, lapilli tuffs, and crystal-rich eutaxitic lapilli tuffs, all intruded by porphyritic rocks. This lithological diversity indicates a complex succession of volcanic and sedimentary events.

Three Facies Associations were recognized. Facies Associations 1 and 2 indicate a continental lacustrine basin environment, in transition from fluvial to low-energy lacustrine sedimentation. Facies Association 3 is regarded as belonging to another event and is tentatively interpreted as part of a caldera lithofacies.

Zircon analysis from lithofacies 3 yielded an age of 189.5 ± 2.2 Ma, providing a precise date for the crystallization of the volcanic components, and correlating the coeval sedimentation with the Early Jurassic (Pliensbachian). The presence of zircons inherited from the Cambrian and Silurian suggests the assimilation of older basement material during volcanic processes.

A new plant fossil association is recorded from the Puesto Piris Formation, with equisetalean stems and vegetative and reproductive structures of conifers. It is referred to the Sinemurian-Pliensbachian boundary on account of the U/Pb zircon age reported here. The pollen grain *Inaperturopollenites indicus* has been identified in our association and has also been recorded in other Lower Jurassic units.

The Marifil Complex, in particular the Puesto Piris Formation, is a unit of potential interest for the study of the Lower Jurassic taphofloras of Patagonia. In view of these incidental findings, future field trips may provide additional elements for comparison with other Jurassic units in Argentina and elsewhere in Gondwana, contributing to a better understanding of the paleofloristic evolution of the Early Jurassic.

ACKNOWLEDGMENTS

Authors express their gratitude to Dr. Susana Damborenea, Invited Editor, and the reviewers Dr. Miguel Haller, and an anonymous reviewer for their valuable suggestions and corrections which have greatly improved this manuscript. The

English writing was reviewed by Rosemary Scoffield.

REFERENCES

- Arguijo, M.H. and Volkheimer, W. 1985. Palinología de la Formación Piedra Pintada, Jurásico Inferior, Neuquén, República Argentina. Descripciones sistemáticas. *Revista Española de Micropaleontología* 17(1): 65-92.
- Arrondo, O.G. and Petriella, B. 1980. Alicurá, una nueva localidad plantífera liásica de la provincia de Neuquén, Argentina. *Ameghiniana* 17: 200-215.
- Benedini, L., Barros, M., Pavón Pivetta, C., Stremel, A., Gregori, D.A., Marcos, P., Bahía M., Scivetti, N., Strazzere, L. and Gerales, M. 2022. New insights into the Jurassic polyphase strain partition on the Patagonian back-arc; constraints from structural analysis of ancient volcanic structures. *Tectonophysics* 836: 229430.
- Branney, M.J. and Kokelaar, P. 2002. Pyroclastic density currents and the sedimentation of ignimbrites. *Geological Society, Memoir* 27, 143 p, London.
- Busteros, A.G., Giacosa, R.E., Lema, H.A. and Zubía, M.A. 1998. Hoja Geológica 4166-IV Sierra Grande. Servicio Geológico Minero Argentino, Instituto de Geología y Recursos Minerales, Boletín 241: 1-75, Buenos Aires.
- Caminos, R. 2001. Hoja Geológica 4166-I, Valcheta, provincia de Río Negro. Servicio Geológico Minero Argentino, Boletín 310: 1-78, Buenos Aires.
- Cas, R.A.F. and Wright, J.V. 1987. Volcanic successions: Modern and ancient. A geological approach to processes, products and successions. Allen and Unwin, 518 p., London.
- Chernicoff, C.J., Gozalvez, M.R., Santos, J.O. and Mc Naughton, N.J. 2017. Edad U/Pb SHRIMP en circones y caracterización de la Riolita Punta del Agua, sector centro oriental de la provincia de Río Negro, Argentina: nueva evidencia de la compresión jurásica inferior en la Patagonia oriental. 20° Congreso Geológico Argentino, Actas 15: 14-15, San Miguel de Tucumán.
- Chiarella, D. 2011. Sedimentology of Pliocene-Pleistocene mixed (lithoclastic-bioclastic) deposits in southern Italy (Lucanian Apennine and Calabrian Arc): depositional processes and palaeogeographic frameworks. PhD Thesis (unpublished), 216 p. University of Basilicata.
- Chiarella D., Longhitano S.G. and Muto F. 2009. Sedimentary features of Lower Pleistocene mixed lithoclastic-bioclastic deposits in a fault-bounded basin, Catanzaro Basin (Southern Italy). *Fist Geotitalia* 3: 399, Rimini.
- Chiarella, D., Moretti, M., Longhitano, S.G. and Muto, F. 2016. Deformed cross-stratified deposits in the Early Pleistocene tidally-dominated Catanzaro strait-fill succession, Calabrian Arc (Southern Italy): triggering mechanisms and environmental significance. *Sedimentary Geology* 344: 277-289.
- Chiarella, D., Longhitano, S.G. and Tropeano, M. 2017. Types of mixing and heterogeneities in siliciclastic-carbonate sediments. *Marine and Petroleum Geology* 88: 617-627.
- Cohen, K.M., Finney, S.C., Gibbard, P.L. and Fan, J.-X. 2013 (updated). The ICS International Chronostratigraphic Chart. *Episodes* 36: 199-204.
- Cortés, J.M. 1979. Primeros afloramientos de la Formación Sierra Grande en la provincia del Chubut. 7° Congreso Geológico Argentino, Actas 1: 481-487, Buenos Aires.
- Cortés, J.M. 1981. El sustrato precretácico del extremo noreste de la provincia del Chubut. *Revista de la Asociación Geológica Argentina* 36(3): 217-235.
- Costa, R.V., Trouw, R.A.J., Mendes, J.C., Gerales, M., Tavora, A., Nepomuceno, F. and Araújo Jr., E.B., 2017. Proterozoic evolution of part of the Embu Complex, eastern São Paulo state, SE Brazil. *Journal of South American Earth Sciences* 79: 170-188.
- Cox, K.G. 1992. Karoo igneous activity, and the early stages of the breakup of Gondwanaland. Geological Society, London, Special Publications 68(1): 137-148.
- Díaz-Martínez I, González, S.N. and de Valais S. 2017. Dinosaur footprints in the Early Jurassic of Patagonia (Marifil Volcanic Complex, Argentina): biochronological and palaeobiogeographical inferences. *Geological Magazine* 154(4): 914-922.
- Dunham, R.J. 1962. Classification of carbonate rocks according to depositional textures. *Memoirs, American Association of Petroleum Geologists* 1: 108-121.
- Encarnación, J., Fleming, T.H., Elliot, D.H. and Eales, H.V. 1996. Synchronous emplacement of Ferrar and Karoo dolerites and the early breakup of Gondwana. *Geology* 24: 535-538.
- Escapa, I.H., Cúneo, N.R. and Cladera, G. 2008. New evidence for the age of the Jurassic Flora from Cañadón del Zaino, Sierra de Taquetrén, Chubut. *Ameghiniana* 45: 633-637.
- Falco, J.I., Hauser, N., Olivera, D., Bodnar, J. and Reimold, W.U. 2021. A multi-proxy study of the Cerro Piche Graben-A Lower Jurassic basin in the central North Patagonian Massif, Argentina. *Journal of South American Earth Sciences* 109: 103287.
- Féraud, G., Alric, V., Fornari, M., Bertrand, H. and Haller, M. 1999. ⁴⁰Ar/³⁹Ar dating of the Jurassic volcanic province of Patagonia: Migrating magmatism related to Gondwana break-up and subduction. *Earth Planetary Science Letter* 172 (1): 83-96.
- Ferello, R. 1947. Los depósitos plantíferos de Piedra del Águila (Neuquén) y sus relaciones. *Boletín de Informaciones Petroleras* 278: 248-261.
- Franchi, M., Ardolino, A. and Remesal, M. 2001. Hoja Geológica 4166 III, Cona Niyeu, provincia de Río Negro. Servicio Geológico Minero Argentino, Boletín 262:1-114, Buenos Aires.
- Gerales, M.C., Almeida, B.S., Tavares Jr., A., Dussin, I. and Chemale, F. 2015. U/Pb and Lu-Hf calibration of the new LA-ICP-MS Multilab at Rio de Janeiro State University. *Geoanalysis*, Leoben.
- Giacosa, R. 1987. Caracterización de un sector del basamento metamórfico-migmático en el extremo suroccidental del Macizo Nordpatagónico, provincia de Río Negro, Argentina. 10° Congreso Geológico Argentino

- no, Actas 3: 51-5, San Miguel de Tucumán.
- Gianni, G.M., Dávila, F.M., Echaurren, A., Fennell, L., Tobal, J., Navarrete, C. and Giménez, M. 2018. A geodynamic model linking Cretaceous orogeny, arc migration, foreland dynamic subsidence and marine ingression in southern South America. *Earth-Science Reviews* 185: 437-462.
- Gianni, G.M., Navarrete, C. and Spagnotto, S. 2019. Surface and mantle records reveal an ancient slab tear beneath Gondwana. *Scientific Reports* 9 (1): 19774.
- Gianni, G.M., Likerman, J., Navarrete, C.R., Gianni, C.R. and Zlotnik, S. 2023. Ghost-arc geochemical anomaly at a spreading ridge caused by supersized flat subduction. *Nature Communications* 14 (1): 2083.
- Gnaedinger, S.C. and Zavattieri, A.M. 2017. Nuevos registros paleobotánicos de la Formación Nestares (Jurásico Temprano), extremo austral de la Cuenca Neuquina, Argentina. *Revista del Museo Argentino de Ciencias Naturales n.s.* 19(2): 101-112.
- González, S.N., Greco, G., González, P.D., García, V., Llambías, E., Sato, A.M. and Díaz, P. 2013. Geología de un enjambre longitudinal de diques mesosilícicos en la Patagonia norte. 2° Simposio sobre Petrología Ígnea y Metalogénesis Asociada, Actas: 43, San Luis.
- González, S.N., Greco, G.A., Sato, A.M., González, P.D., Llambías, E.J., Díaz Martínez, I., de Valais, S. and Serra Varela, S. 2017a. Revisión estratigráfica del Complejo Volcánico Marifil. 20° Congreso Geológico Argentino, ST(1): 72-77, San Miguel de Tucumán.
- González, S.N., Greco, G.A., Sato, A.M., Llambías, E., Basei, M.A.S., González, P.D. and Díaz, P.E. 2017b. Middle Triassic trachytic lava flows associated with coeval dyke swarm in the North Patagonian Massif: A postorogenic magmatism related to extensional collapse of the Gondwanide orogen, *Journal of South American Earth Sciences* 75: 134-143.
- González, S.N., Greco, G.A., Galetto, A., Bordes, S., Basei, M.A., Parada, M.N., Giacosa, R. and Pons, M.J. 2022. A multi-method approach to constrain the age of eruption and post-depositional processes in a Lower Jurassic ignimbrite from the Marifil Volcanic Complex, eastern North Patagonian Massif. *Journal of South American Earth Sciences* 114: 103688.
- Herbst, R. 1966. Revisión de la flora liásica de Piedra Pintada, Provincia de Neuquén, Argentina. *Revista del Museo de La Plata, n.s., Sección Paleontología* 30: 27-53.
- Hesse, R. 1989. Silica diagenesis: origin of inorganic and replacement cherts. *Earth-Science Reviews* 26: 253-284.
- Linares, E. 1977. Catálogo de edades radiométricas determinadas para la República Argentina: I-Años 1974-1976 y Catálogo de edades radiométricas realizadas por INGEIS y sin publicar, 1-Años 1972-1974. *Publicaciones Especiales de la Asociación Geológica Argentina, Serie B (Didáctica y Complementaria)* 4: 1-38.
- Lizuaín, A. 1983. Descripción Geológica de la Hoja 38 j, Salinas del Gualicho. Servicio Geológico Nacional, Boletín 195, 1-48, Buenos Aires.
- Longhitano, S.G., Chiarella, D., Di Stefano, A., Messina, C., Sabato, L. and Tropeano, M., 2012. Tidal signatures in Neogene to Quaternary mixed deposits of southern Italy straits and bays. *Sedimentary Geology* 279: 74-96.
- Malvicini, L. and Llambías, E. 1974. Geología y génesis del depósito de manganeso Arroyo Verde, provincia del Chubut, República Argentina. 5° Congreso Geológico Argentino, Actas 2: 185-202, Villa Carlos Paz.
- Martínez, M.A., Quattrocchio, M.E. and Sarjeant, W.A.S. 2001. Análisis palinoestratigráfico de la Formación Lajas, Jurásico Medio de la Cuenca Neuquina, Argentina. *Revista Española de Micropaleontología* 33(1): 33-60.
- Martínez, M.A., Quattrocchio, M.E. and Prámparo, M.B. 2005. Análisis palinológico de la Formación Los Molles, Grupo Cuyo, Jurásico medio de la cuenca Neuquina, Argentina. *Ameghiniana* 42(1): 67-92.
- McPhie, J., Doyle, M. and Allen, R. 1993. Volcanic textures: A guide to the interpretation of textures in volcanic rocks. Centre for ore deposit and exploration studies, Tasmania University Press, 196 p., Tasmania.
- Miall, A.D. 2006. The geology of fluvial deposits. *Sedimentary Facies, Basin Analysis, and Petroleum Geology*. Springer, 582 p., Berlin.
- Morel, E.M., Ganuza, D.G., Artabe, A.E. and Spalletti, L.A. 2013. Revisión de la paleoflora de la Formación Nestares (Jurásico Temprano), provincias del Neuquén y Río Negro, Argentina. *Ameghiniana* 50(5): 493-508.
- Navarrete, C., Gianni, G., Encinas, A., Márquez, M., Kamerbeek, Y., Valle, M. and Folguera, A. 2019a. Triassic to Middle Jurassic geodynamic evolution of southwestern Gondwana: From a large flat-slab to mantle plume suction in a rollback subduction setting. *Earth-Science Reviews* 194: 125-159.
- Navarrete, C., Gianni, G., Christiansen, R., Kamerbeek, Y., Periale, S. and Folguera, A. 2019b. Jurassic intraplate contraction of southern Patagonia: the El Tranquilo anticline area, Deseado Massif. *Journal of South American Earth Sciences* 94: 102224.
- Navarrete Granzotto, C.R., Gianni, G.M., Tassara, S., Zaffarana, C.B., Likerman, J., Márquez, M., Wostbrock J., Planavsky, N., Tardani, D. and Perez Frassetto, M.J. 2024. Massive Jurassic slab break-off revealed by a multidisciplinary reappraisal of the Chon Aike silicic large igneous province. *Earth Science Reviews* 249: 104651.
- Navarro, E.L., Astini, R.A., Belousova, E., Guler, M.V. and Gehrels, G. 2015. Detrital zircon geochronology and provenance of the Chubut Group in the northeast of Patagonia, Argentina. *Journal of South American Earth Sciences*, 63: 149-161.
- Noetinger, S., Pujana, R.R., Burrieza, A. and Burrieza, H.P. 2017. Use of UV-curable acrylates gels as mounting media for palynological samples. *Revista del Museo Argentino de Ciencias Naturales* 19(1): 19-23.
- Núñez, E., Bachmann, E., Ravazzoli, I., Britos, A., Franchi, M., Lizuaín, A., and Sepúlveda, E. 1975. Rasgos geológicos del sector oriental del Macizo de Somuncurá, Provincia de Río Negro, República Argentina. 2° Congreso Iberoamericano de Geología Económica, Actas 4: 247-266, Buenos Aires.
- Olivera, D.E. 2015. Estudio palinológico y palinofacies del Jurásico Me-

- dio y Tardío de la Provincia de Chubut: Sistemática, Bioestratigrafía y Paleoecología. Tesis Doctoral, Universidad Nacional del Sur (inédita), 285 p., Bahía Blanca.
- Olivera, D.E., Martínez, M.A., Zavala, C. and Ballent, S.C. 2010. Los depósitos oxfordiano-kimmeridgianos de la Formación Lotena: nuevas perspectivas en la estratigrafía del Jurásico Tardío de la Cuenca Neuquina, Argentina. *Ameghiniana* 47(4): 479-500.
- Page, N.F. 1987. Descripción Geológica de la Hoja 43g, Bajo de la Tierra Colorada, provincia del Chubut. Servicio Geológico Nacional, Boletín 200: 1-81, Buenos Aires.
- Pankhurst, R.J. and Rapela, C.R. 1995. Production of Jurassic rhyolite by anatexis of the lower crust of Patagonia. *Earth Planetary Science Letter* 134(1): 23-36.
- Pankhurst, R.J., Riley, T.R., Fanning, C.M. and Kelley, S.P. 2000. Episodic silicic volcanism in Patagonia and the Antarctic Peninsula: chronology of magmatism associated with the break-up of Gondwana. *Journal of Petrology* 41 (5): 605-625.
- Pavón Pivetta, C., Gregori, D., Benedini, L., Garrido, M., Strazzere, L., Gerales, M., Costa dos Santos, A. and Marcos, P. 2020. Contrasting tectonic settings in Northern Chon Aike Igneous Province of Patagonia: subduction and mantle plume-related volcanism in the Marifil formation. *International Geology Review* 62 (15): 1904-1930.
- Pavón Pivetta, C., Benedini, L., Marcos, P., Cocola, M.A., Barros, M.V., Gregori, D., Strazzere, L., Costa dos Santos, A. and Gerales, M.C. 2024. Characterization of Arroyo Verde Epithermal Deposit: Paragenesis, Mineral Geochemistry, Geochronology and Fluid Inclusions in Lower Chon Aike Volcanism, Argentina. *Journal of Earth Science* 35(1): 62-84.
- Pugliese, F.E., Pugliese, L.E., Dahlquist, J.A., Basei, M.A.S. and Dopico, C.I.M. 2021. Intermediate sulfidation epithermal Pb-Zn (\pm Ag \pm Cu \pm In) and low sulfidation Au (\pm Pb \pm Ag \pm Zn) mineralization styles in the Gonzalito polymetallic mining district, North Patagonian Massif. *Journal of South American Earth Sciences* 110: 103388.
- Ramos, V. 1975. Geología del sector oriental del Macizo Norpatagónico entre Aguada Capitán y la Mina Gonzalito, provincia de Río Negro. *Revista de la Asociación Geológica Argentina* 30 (3): 274-285.
- Rapela, C.W. and Pankhurst, R.J. 1993. El volcanismo riolítico del nordeste de la Patagonia: Un evento meso-jurásico de corta duración y origen profundo. 12° Congreso Geológico Argentino y 2° Congreso de Exploración de Hidrocarburos, Actas 4: 179-188, Mendoza.
- Riding, J.B. 2021. A guide to preparation protocols in palynology. *Palynology* 45(S1): 1-110.
- Riley, T.R. and Knight, K.B. 2001. Age of pre-break-up Gondwana magmatism. *Antarctic Science* 13(2): 99-110.
- Rubatto, D. 2002. Zircon trace element geochemistry: partitioning with garnet and the link between U-Pb ages and metamorphism. *Chemical Geology* 184 (1-2): 123-138.
- Sagasti, A.J., Morel, E.M., Ganuza, D. and Knight, P.A. 2019. New paleofloristic elements and stratigraphic considerations for the Nestares Formation (Lower Jurassic, Argentina). *Journal of South American Earth Sciences* 94: 102245.
- Spalletti, L., Franzese, J., Morel, E., Zúñiga, A. and Fanning, C.M. 2010. Consideraciones acerca de la sedimentología, paleobotánica y geocronología de la Formación Piedra del Águila (Jurásico Inferior, Neuquén). *Revista de la Asociación Geológica Argentina* 66(3): 305-313.
- Srivastava, S. 1966. Jurassic microflora from Rajasthan, India. *Micropaleontology* 12(1): 87-102.
- Storey, B.C., Leat, P.T. and Ferris, J.K. 2001. The location of mantle-plume centers during the initial stages of Gondwana break-up. In: Ernst, R.E. and Buchan, K.L. (eds.), *Mantle Plumes: Their identification through time*. Geological Society of America Special Papers 352: 71-80.
- Strazzere, L., Gregori, D.A., Benedini, L., Marcos, P., Barros, M.V., Gerales, M.C. and Pavón Pivetta, C. 2019. The Puesto Piris Formation: Evidence of basin-development in the North Patagonian Massif during crustal extension associated with Gondwana breakup. *Geoscience Frontiers* 10(1): 299-314.
- Strazzere, L., Pavón Pivetta, C., Gregori, D.A., Benedini, L., Gerales, M.C. and Barros, M.V. 2022. The Marifil Volcanic Complex at Sierra de Pailemán: implications for the Early Jurassic magmatic evolution of the Eastern North Patagonian Region. *International Geology Review* 64(6): 844-866.
- Valvano, J.A. 1954. Génesis de los yacimientos de Hierro de Sierra Grande. *Revista de la Asociación Geológica Argentina* 9(4): 193-209.
- Volkheimer, W. 1968. Esporas y granos de polen del Jurásico de Neuquén (República Argentina). I. Descripciones sistemáticas Asociaciones microfóricas, aspectos paleoecológicos y paleoclima. *Ameghiniana* 5(9): 333-370.
- Volkheimer, W. 1969. Esporas y granos de polen del Jurásico de Neuquén (República Argentina). II. Asociaciones microfóricas, aspectos paleoecológicos y paleoclima. *Ameghiniana* 6(2): 127-145.
- Volkheimer, W. 1971. Algunos adelantos en la microbioestratigrafía del Jurásico en la Argentina y comparación con otras regiones del hemisferio austral. *Ameghiniana* 8(3-4): 341-355.
- Volkheimer, W. 1972. Estudio palinológico de un carbón caloviano de Neuquén y consideraciones sobre los paleoclimas jurásicos de la Argentina. *Revista del Museo de la Plata n. s.* 6(37): 101-157.
- Volkheimer, W. and Melendi, D.L. 1976. Palinomorfos como fósiles guía (3a parte). Técnicas del laboratorio palinológico. *Revista minera de Geología y Mineralogía* 34: 19-30.
- Volkheimer, W. and Papú, O.H. 1993. Una microflora del Triásico Superior de la Cuenca Malargüe, localidad Llantenes, provincia de Mendoza, Argentina. *Ameghiniana* 30(1): 93-100.
- Wei, W., Azmy, K. and Zhu, X. 2022. Impact of diagenesis on reservoir quality of the lacustrine mixed carbonate-siliciclastic-volcaniclastic rocks in China. *Journal of Asian Earth Sciences* 233, 105265.
- Whitney, D.L. and Evans, B.W. 2010. Abbreviations for names of rock-forming minerals. *American Mineralogist* 95(1): 185-187.
- Ylláñez, E. 1987. Descripción geológica de la Hoja 42g, Telsen, provincia

- del Chubut: Servicio Geológico Nacional, Boletín 208: 1-55, Buenos Aires.
- Zanettini, J.C. 1981. La Formación Sierra Grande (provincia de Río Negro). Revista de la Asociación Geológica Argentina 36(2): 160-179.
- Zavattieri, A.M. 1986. Estudio palinológico de la formación Potrerillos (Triásico) en su localidad tipo, Cuenca Cuyana (Provincia de Mendoza, Argentina) Parte I. Esporas triletes y monoletes. Revista Española de Micropaleontología 18(2): 247-294.
- Zavattieri, A.M. 1987. Estudio palinológico de la Formación Potrerillos (Triásico) en su localidad tipo, Cuenca Cuyana (Provincia de Mendoza, Argentina): Parte II. Granos de polen. Aspectos estadísticos. Correlación palinoestratigráfica. Revista Española de Micropaleontología 19(2): 173-213.
- Zavattieri, A.M. and Volkheimer, W. 2003. Palynostratigraphy and paleoenvironments of Early Jurassic strata (Nestares Formation) in northern Patagonia, Argentina. Part 1. Terrestrial species. Ameghiniana 40: 545-558.
- Zavattieri, A.M., Rosenfeld, U. and Volkheimer, W. 2008. Palynofacies analysis and sedimentary environment of Early Jurassic coastal sediments at the southern border of the Neuquén Basin, Argentina. Journal of South American Earth Sciences 25: 227-245.